Identification of genetic loci associated with primary angle-closure glaucoma in the basset hound

Dina F. Ahram,[1,2] Amy C. Cook,[2] Helga Kecova,[2] Sinisa D. Grozdanic,[3] Markus H. Kuehn[1,2]

[1]*Interdisciplinary Graduate Program in Genetics, Iowa City, IA;* [2]*Department of Ophthalmology and Visual Sciences, Iowa City, IA;* [3]*Animal Eye Consultants of Iowa, North Liberty, Iowa*

Purpose: Primary angle-closure glaucoma (PACG) in dogs is usually caused by the gradual collapse of the iridocorneal angle and cleft, eventually leading to aqueous humor (AH) outflow obstruction. The condition occurs in several breeds of dogs and the prognosis for affected animals is typically poor. We have identified several basset hound (BH) pedigrees, as well as unrelated cases with characteristic PACG that in many aspects recapitulates PACG in human patients. The goal of this study was to utilize the BH PACG model to characterize the genetics of PACG, and potentially discover genetic factors contributing to PACG in humans and animals.

Methods: We conducted a genome-wide logistic regression test for association using 37 PACG cases and 41 unaffected controls. Population stratification and cryptic relatedness were assessed using a multidimensional scaling analysis. The expression of two candidate genes within the target tissues of the BH eye was assessed by immunohistochemistry.

Results: We report significant associations at two novel loci, specifically BICF2P31912 in *COL1A2* on chromosome 14 with a per-allele odds ratio (OR, 95% confidence interval [CI]) of 3.35 (1.73–6.51), P_{genome}=3.6×10^{-4}; and BICF2P893476 residing in proximity to *RAB22A* on chromosome 24 with a per-allele OR (95% CI) of 3.93 (1.78–8.66), P_{genome}=4.9×10^{-4}. COL1A2 and RAB22A demonstrated widespread expression throughout the eye and were prominently noted in the ciliary body (CB), trabecular meshwork (TM), and iris.

Conclusions: Our finding of two genetic associations supports the potential segregation of PACG risk-conferring variants in the BH. The genetic associations identified may contribute to mechanisms underlying the pathogenesis of PACG, which remain to be elucidated.

Glaucoma is the third most frequent cause of blindness worldwide [1], and is known to affect both humans and numerous dog breeds. Several types of glaucoma exist, including primary angle-closure glaucoma (PACG), which is three times more prevalent in humans of Asian descent than in European populations [2-4]. In human patients, PACG is typically caused by the collapse of the iridocorneal angle due to the anterior movement of the iris root, which in turn blocks the outflow of aqueous humor (AH) through the trabecular meshwork (TM). Conversely, clinical investigation of hereditary PACG in the basset hound (BH) has revealed progressive collapse of the ciliary cleft (CC) and TM region in association with a gradual increase in intraocular pressure (IOP), which becomes statistically significant (20–24 mmHg) by 20 months of age [5]. The condition is marked by retinal ganglion cell death, retinal neuroinflammation, axonal degeneration, and cupping of the optic nerve head secondary to increased IOP [6].

BHs display glaucomatous neuropathy similar to that observed in human PACG patients. Progressive deficits in

Correspondence to: Markus H Kuehn, The University of Iowa, Ophthalmology and Visual Sciences 4184 MERF, Iowa City, IA 52242; Phone: (319) 335-9565; FAX: (319) 335-6641; email: markus-kuehn@uiowa.edu

retinal ganglion cell function are noted by pattern electroretinography (pERG) in the basset. Additionally, axonal degeneration and prominent structural changes to the optic nerve head are observed in the advanced stages of the disease. The frequent absence of early symptoms makes PACG difficult to detect and places a large proportion of both human and canine cases at risk for blindness.

There is strong evidence that human PACG is a complex disease with a significant underlying genetic component [7,8]. Family history is one of the major risk factors for PACG and heritability estimates have shown a 3.7-fold increase in disease risk among siblings compared to the general population [9,10]. Despite extensive research efforts, the genetic basis of PACG is still incompletely understood. Several candidate genes for human PACG have been identified so far. A recent genome-wide association study (GWAS) has reported three susceptibility loci in an Asian population [8]. Association studies have also suggested the involvement of several single-nucleotide polymorphisms (SNPs) in the matrix metalloproteinase-9 (*MMP9*; OMIM 120361) in both Chinese and Caucasian populations [11,12]. Some of these findings were not reproducible in other ethnic populations, however, which suggests the genetic heterogeneity of PACG in human populations [13].

Similarly, data regarding the genetics of glaucoma in dogs is sparse. Genetic investigation of primary open-angle glaucoma (POAG) in a beagle colony revealed a single locus on chromosome 20 harboring the gene *ADAMTS10* [14]. A GWA analysis of a late-onset form of PACG described in a Dandie Dinmont terrier cohort has also led to the identification of a novel susceptibility locus on canine chromosome 8 [15]. The locus shares synteny to a region on human chromosome 14q, which harbors several genes associated with POAG and primary congenital glaucoma [16].

BHs are among several breeds of dogs that are predisposed to developing glaucoma [17]. A total of 5.44% of all BHs treated in teaching hospitals presented with glaucoma, representing a significantly higher fraction than most breeds [18]. Unfortunately, treatment options are limited and affected animals often develop bilateral blindness. Other breeds likely to be affected include the American cocker spaniel, wire fox terrier, and Boston terrier [18]. The observation of multiple breeds at risk for developing the same form of the disease may possibly indicate that a shared founder mutation has been preserved with selective breeding. If true, the identification of a significant PACG risk-conferring variant in the BH may serve to determine the risk of disease in other breeds sharing the same mutation.

We have identified several BH pedigrees, as well as unrelated dogs with characteristic PACG that closely recapitulates the phenotype observed in human patients. All affected dogs present with a comparable disease phenotype. Our goal was to identify valid genetic associations that confer risk to PACG by using the BH as a genetic model. The findings of this study are anticipated to provide valuable insight into the pathophysiology and genetic mechanisms underlying canine PACG. The identification of genetic risk variants in dogs can assist in reducing the incidence of PACG in susceptible breeds using selective breeding.

METHODS

Animals and clinical presentation: All animal studies were conducted in accordance with the Association for Research in Vision and Ophthalmology (ARVO) statement for use of animals in ophthalmic and vision research. The procedures conducted were approved by the respective University of Iowa and Iowa State University Committees on animal care and use. Our GWA investigation of PACG in cases versus controls included unrelated as well as related animals derived from six pedigrees with clinically confirmed PACG. All animals included were examined by a veterinary ophthalmologist as described previously [5].

Examination of the anterior segment was performed by gonioscopy using a gonioscopy lens (Koeppe; Inc.), a hand-held Kowa SL-15 slit lamp (Kowa Optimed Inc., Torrance, CA) and a high-frequency ultrasonography unit with a 35-MHz probe (E-Technologies, Bettendorf, IA). Additionally, gonioscopy photography was performed using a gonioscopy lens and a handheld retinal camera (RetCam; Massie Research Laboratories, Pleasanton, CA). Collapse of the iridocorneal angle was considered the most significant determinant of glaucoma diagnosis. Examination of the anterior segment was performed by gonioscopy using a gonioscopy lens (Koeppe; Ocular Instruments Inc., Bellevue, WA), a hand-held Kowa SL-15 slit lamp (Kowa Optimed Inc., Torrance, CA) and a high-frequency ultrasonography unit with a 35-MHz probe (E-Technologies, Bettendorf, IA). Additionally, gonioscopy photography was performed using a gonioscopy lens and a handheld retinal camera (RetCam; Massie Research Laboratories, Pleasanton, CA). Animals with possible secondary glaucoma or other confounding ocular conditions were excluded from the study. Control animals were at least four years of age, and had a normal iridocorneal angle and cleft conformation observed by gonioscopy and high frequency ultrasound to ensure accurate diagnosis of their unaffected status. Additionally, globes (n=6) from animals that underwent enucleation due to clinical glaucoma refractive to medical or surgical treatment were submitted for histopathology and further evaluation.

Genetic analysis: Whole blood was collected from 37 clinically confirmed glaucoma cases and 41 unaffected controls with the owners' consent. Genomic DNA was extracted from EDTA-stabilized whole blood samples using the Qiagen DNeasy blood and tissue kit (Qiagen, Hilden, Germany). DNA samples were eluted with deionized water and stored at −20°C. Seventy-eight samples were genotyped using the Illumina CanineHD BeadChip (Illumina, San Diego, CA), which contains 172,000 markers placed on a CanFam2.0 reference sequence.

Prior to GWA analysis, preliminary quality control assessment of genotyped SNPs was conducted using PLINK [19] to remove genotype errors and uninformative data. All SNPs were subjected to strict quality control (QC) criteria: SNPs with a minor allele frequency <1%, a call rate <95%, a rate of missing genotype >10%, and those that departed from Hardy–Weinberg equilibrium (*P* value <0.001) were excluded from the analysis. All samples had less than a 5% missing genotype rate.

Pairwise clustering based on the GWA proportion of alleles shared identical by state (IBS) between any two individuals was performed to account for increased relatedness.

All sample pairs were ensured to display an IBS relatedness value (pi-hat) <0.9. Population stratification was assessed using a multidimensional scaling analysis (MDS), with three-dimensional components extracted using PLINK [19]. MDS cluster analysis included a selected number of individual animals from each pedigree. To our knowledge, our pedigrees do not share a recent common ancestor and have not been recently interbred. A logistic regression test for GWA was performed. GWA testing was conducted with the inclusion of MDS-based covariates to correct for increased relatedness and population stratification by clustering individual samples based on their pedigrees of origin. The genomic-control inflation factor (λgc) was applied to the test statistic following MDS adjustment by three components. The odds ratio (OR) and 95% confidence interval (CI) were estimated for an additive effect model of allele dosage in the context of logistic regression. The threshold for genome-wide significance was set by permutation testing using 1,000 permutations. For haplotype definitions we performed linkage disequilibrium (LD)-clumping (settings; $r2=0.8$, $p1=0.001$, $p2=0.01$, distance-kb=500) using PLINK v1.07 [19]. Quantile-quantile (Q-Q) and Manhattan plots of $-\log_{10}$ p values were constructed using RStudio (2012).

Tissue processing and histological analyses: Eyes derived from affected and unaffected animals were fixed immediately following enucleation in 4% paraformaldehyde. Tissues were dehydrated then subjected to paraffin embedding using standard procedures. Globes were embedded and 4 µm sagittal sections were made using a rotary microtome. Tissue sections were deparaffinized in xylene for 20 min then hydrated in decreasing ethanol concentration for 5 min at each concentration. Heat-assisted antigen retrieval was performed using 10mM citrate buffer (pH 6.0) for 10 min at 95–100 °C. Blocking of endogenous peroxidase activity was achieved by treating sections with 2% H_2O_2-methanol solution for 20 min at room temperature. Sections were blocked in 5% normal goat serum/1% bovine serum albumin (BSA) solution in 1X Tris-buffered saline (TBS) for 1 h at room temperature then incubated overnight at 4 °C in primary rabbit anti-*COL1A2* (1:100) or rabbit anti-RAB22A (1:100) in 1X TBS (Protein-tech™, Chicago, IL). Sections were treated with biotinylated secondary anti-rabbit immunoglobulin G (IgG) antibody (1:100; Vector, Burlingame, CA). Color development was achieved using an Avidin/Biotinylated–peroxidase Complex VECTASTAIN® ABC kit (Vector, Burlingame, CA) by direct application to tissue sections for 2 min. Sections were dehydrated, cleared in xylene and mounted using Permount™ mounting media (Thermo Fisher Scientific Inc., Waltham, MA). Immunohistochemical staining was evaluated at the light microscopic level.

To evaluate collagen localization, tissue sections were stained with Picrosirius red stain (Polysciences Inc. Warrington, PA) and counterstained with Mayer's Haematoxylin stain (Sigma-Aldrich®, St. Louis, MO) using standard procedures. Negative control tissue sections were generated by staining with Mayer's Haematoxylin stain only. Picrosirius red–stained sections were examined using polarizing microscopy and a color wavelength (from yellow-orange to deep red) indicative of collagen fiber thickness was noted in collagen containing regions.

RESULTS

Animals and clinical presentation: We previously described that the development of elevated IOP and subsequent vision loss is correlated to the gradual narrowing of the irido-corneal angle, resulting in complete angle closure in all affected animals. In concordance with these findings, all cases included in this study displayed completely collapsed iridocorneal angles and CCs confirmed using high-resolution ultrasound (HRUS) and gonioscopy examination. Angle collapse was observed in association with notable IOP elevation of at least 25 mmHG. All unaffected control animals displayed normal IOPs, and had normal appearing iridocorneal angles and CCs by gonioscopy and HRUS, respectively.

Genome-wide association mapping: We performed GWA analysis of PACG in the BH by analyzing clinically confirmed cases and controls to identify genetic variants associated with PACG. The genotyping success rate was set to a value >90%. Prior to GWA analysis, a strict QC criterion was applied to all genotyped SNPs. Out of 172,105 SNPs, we excluded 16,073 (9.33%) uncalled genotypes, 201 (0.12%) markers due to the departure from Hardy–Weinberg equilibrium, 5,739 (3.33%) due to a call rate below 95%, and 37,636 (21.87%) non-informative markers due to a minor allele frequency below 1%. In total, 112,456 SNPs were included in the analysis following QC testing.

All samples analyzed for the presence of excess proportion of alleles shared IBS revealed a pi-hat value <0.9 and were therefore included in the analysis. To account for population stratification and reduce the confounding effect of subject relatedness, an MDS analysis of all 78 samples was conducted. The utilization of pedigree-based MDS clustering of samples as a test statistic covariate has proven successful at reducing the confounding effect of relatedness in other research studies and as such was adopted in our analysis [20,21]. A scatter plot revealing pedigree-based clusters was generated for 3 MDS components (Figure 1). The MDS plot illustrates the formation of six clusters, which appeared to be influenced by the samples' pedigrees of origin, as follows:
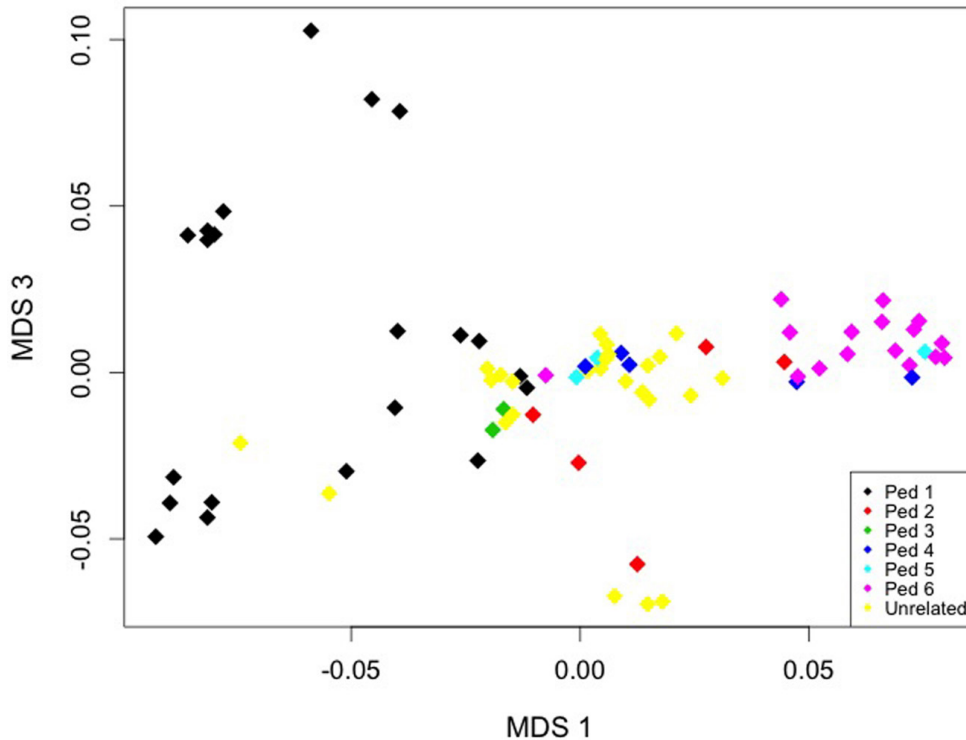
Figure 1. Multidimensional scaling analysis (MDS) scatter plot of cases and controls plotted for the first three MDS dimensions to correct for relatedness and population stratification. Each dot represents a specific dog. Related and unrelated samples are shown clustered according to their affiliation with 6 basset hound (BH) primary angle-closure glaucoma (PACG) pedigrees. The group of unrelated dogs is seen randomly distributed among all pedigree derived samples.

pedigree 1: 21 samples, 14 unaffected, 7 affected; pedigree 2: 5 samples, all affected; pedigree 3: 2 samples, all unaffected;, pedigree 4: 5 samples, 2 unaffected, 3 affected; pedigree 5: 3 samples, 2 affected, 1 unaffected; pedigree 6: 17 samples, 8 unaffected, 9 affected; and unrelated samples: 25 samples, 13 unaffected, 12 affected. Overall, our samples comprised 28 males (14 unaffected, 14 affected) and 50 females (27 unaffected, 23 affected). The group of unrelated samples appeared randomly distributed among the six-pedigree-derived sample clusters. Logistic regression GWA testing was conducted with the inclusion of MDS-generated covariates. An inflation factor ($\lambda_{no\ correction}$=1.30, χ^2=1.33) was calculated before covariate adjustment. Q-Q scatter plots of the −log10 (p values) expected under the null hypothesis of no genetic association versus the observed −log10 (p values) are shown for all subjects before (A) as well as following correction for sample relatedness (B; Figure 2A,B). In the absence of covariate correction, significant deviation from normal distribution was observed for the generated p values, which demonstrates the strong effects of population stratification that is commonly observed when sampling from a founder population (Figure 2A). Conversely, covariate adjustment by the third MDS dimensional component resulted in a corrected inflation factor ($\lambda_{corrected}$=1, χ^2 =0.93). The scatter Q-Q plot in Figure 2B reveals significant improvement in the initially observed deviation from normal distribution of all p values

generated following covariate correction and illustrates the validity of the method used here to correct for relatedness and population stratification.

We identified two regions in association with PACG in the BH following multiple hypothesis testing correction of raw p values by permutation. The first and most statistically significant association (P_{genome}=0.00036, OR=3.35, $CI_{95\%}$=1.73–6.51) was identified for marker BICF2P31912 on chromosome 14, residing in an intronic region of *COL1A2* (Figure 3). The marker is part of a four SNP locus (Chr14:19,911,001–20,161,348bp) spanning 0.25Mb. The four markers constituting the haplotype displayed complete linkage disequilibrium (LD; *D'*=1, *r²*=1). Notable difference in allele and genotype frequency distribution for BICF2P31912 was observed among cases and controls, (58.1% "G") in cases versus (29.3% "G") in controls (Table 1). The allele and genotype distribution of BICF2P31912 is representative of all SNPs within the locus identified.

To define the associated haplotypes, we performed an LD-based clumping analysis with an LD value of *r²*=0.8. Using a threshold value of significance (0.0001 < p<0.001), the four previously identified markers of BICF2P31912, BICF2S2309101, TIGRP2P188010_rs8723846, and BICF2P316805 were validated for constituting an LD-haploblock while reaching the highest P_{genome} values relative to all

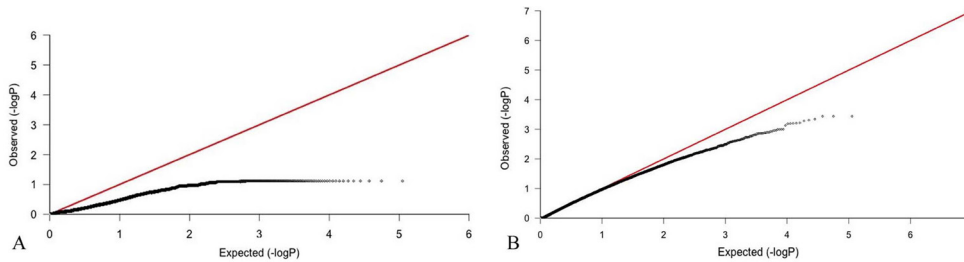Figure 2. Quantile-quantile (Q-Q) plot of primary angle-closure glaucoma (PACG) genome-wide association (GWA) analysis. **A**: Scatter plot of the −log10 (p values) expected under the null hypothesis of no genetic association versus the observed −log10 (p values) for all subjects before correction for population stratification using multidimensional scaling analysis (MDS) generated covariates, and (**B**) following correction for population stratification using MDS generated covariates. A significant improvement in the initially observed deviation from normal distribution of all p values as a result of correcting for relatedness and population stratification effects is observed.

statistically significant markers identified in our GWA analysis. An additional marker (BICF2P1279787) was identified in association with this haploblock ($r2$=0.87) with a reduced p value (P_{genome}=0.00134). The 0.25 Mb locus on Chr14 contains 20 SNPs and 2 CanFam2.0 annotated protein-coding genes, corresponding to the human genes *COL1A2* and *PEG10*.

A second statistically significant association was identified (P_{genome}=0.00049, OR=3.93, $CI_{95\%}$=1.78–8.66) for marker BICF2P893476 on chromosome 24 (Figure 3). The marker is part of a two-SNP locus (Chr24: 43,091,222–43,595,979bp) spanning 0.5 Mb. *RAB22A*, a member of the rat sarcoma (RAS) oncogene family is located within the locus bracketed by the two markers, which display complete LD (D'=1, r^2=1). A notable difference in allele and genotype frequency distribution for BICF2P893476 was observed among cases

and controls, at 37.8% "G" in cases versus 13.4% "G" in controls (Table 2). The allele and genotype distribution of BICF2P893476 is representative of all SNPs within the locus identified.

In addition, five isolated SNPs displaying statistically significant P_{genome} values were identified (Table 3). All variants identified are located in noncoding regions and were not further investigated.

Tissue processing and histological analyses: Immunohistochemical expression of the two statistically significant PACG-associated genes, *COL1A2* and *RAB22A,* was assessed in the dog eye. Staining of COL1A2 and RAB22A in sagittal sections of paraffin-embedded eyes revealed localization of both proteins in various substructures when compared to a negative control where the primary antibody was omitted
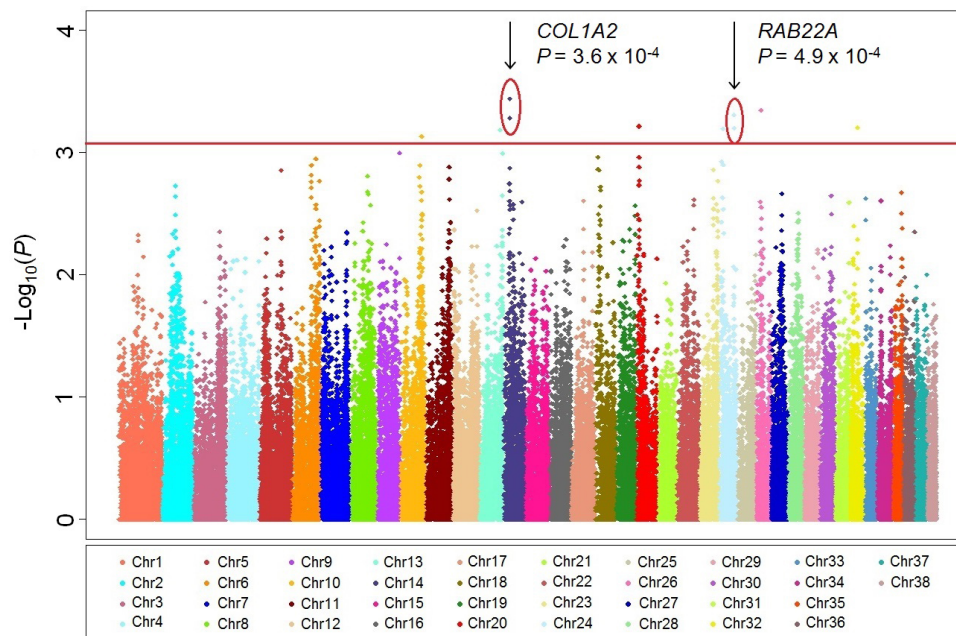

Figure 3. Manhattan plot from the genome-wide association (GWA) analysis of primary angle-closure glaucoma (PACG) in the basset hound (BH) with pedigree-based, multidimensional scaling analysis (MDS)-clustered covariates shows a significant association on chromosome 14. The red line indicates all p values exceeding the permutation adjusted significance threshold of 10^{-4}.

TABLE 1. ASSOCIATION OF ALLELES AND GENOTYPES OF **BICF2P31912** ON CHROMOSOME 14 WITH.

Case/control	Number and Frequency of BICF2P31912 Alleles in PACG		Number and Frequency of BICF2P31912 Genotypes in PACG			Logistic Regression GWA Test				
	G	A	GG	AG	AA	Odds ratio	Stnd error	95% CI L95	95% CI U95	p-value
Cases (37)	43 (58.1)	31 (41.9)	9 (24.3)	25 (67.6)	3 (8.10)	3.35	0.338	1.73	6.51	3.63×10^{-4}
Controls (41)	24 (29.3)	58 (70.7)	3 (7.31)	18 (43.9)	20 (48.8)					

PACG: BICF2P31912 residing within a 4 SNP haplotype showed the highest association with PACG with an odds ratio OR (95% CI)=3.35 (1.73–6.51); p=0.00036. The P_{genome} value was calculated with logistic regression GWA analysis corrected for relatedness and population stratification.

TABLE 2. ASSOCIATION OF ALLELES AND GENOTYPES OF **BICF2P893476** ON CHROMOSOME **24** WITH.

Case/control	Number and Frequency of BICF2P893476 Alleles in PACG		Number and Frequency of BICF2P893476 Genotypes in PACG			Logistic Regression GWA Test				
	G	A	GG	AG	AA	Odds ratio	Stnd error	95% CI L95	95% CI U95	p-value
Cases (37)	28 (37.8)	46 (62.2)	5 (13.5)	18 (48.6)	14 (37.8)	3.93	0.403	1.78	8.66	4.90×10^{-4}
Controls (41)	11 (13.4)	71 (86.6)	0 (0)	11 (26.8)	30 (73.2)					

PACG: BICF2P893476 residing within a 2 SNP haplotype showed the highest association with PACG with an odds ratio OR (95% CI)=3.93 (1.78–8.66); p=0.00049. The P_{genome} value was calculated with logistic regression GWA analysis corrected for relatedness and population stratification.

Chromosome	SNP	Position (bp)	P_{genome}
26	BICF2G630805530	13,936,505	4.5×10^{-4}
20	BICF2P1094598	9,595,282	6.1×10^{-4}
32	BICF2P536453	21,851,662	6.2×10^{-4}
13	BICF2S23423784	58,788,894	6.5×10^{-4}
10	BICF2P528613	62,472,085	7.4×10^{-4}

TABLE 3. ADDITIONAL SNPs IDENTIFIED IN GWA ANALYSIS.

Five single SNPs displaying statistical significance were identified in our case-control GWA analysis of PACG in the BH.

(Figure 4). Prominent COL1A2 localization was noted in the ciliary body (CB) as well as the apical epithelial cell surface of the ciliary processes (Figure 4A). RAB22A similarly localized to the ciliary processes, but revealed faint staining in the CB, indicating reduced localization here. Both proteins displayed minimal localization in the CC and TM (Figure 4B). Localization of COL1A2 was further noted in close proximity to the pigmented epithelium at the apical surface of the iris, whereas RAB22A staining was mostly observed in the stromal region (Figure 4C). In the cornea, COL1A2 was found predominantly located in the stromal regions, whereas, RAB22A staining revealed strong localization in the epithelial layer at the apical surface (Figure 4D). Both proteins revealed localization throughout the retina. COL1A2 showed a slight increase in staining in the outer nuclear layer and retinal ganglion cell layer. RAB22A revealed a strong staining signal in the outer segment and outer plexiform layer (Figure 4E). COL1A2 and RAB22A were also found to localize in the optic nerve when compared to the negative control (Figure 4F). No obvious differences were noted in COL1A2 or RAB22A localization or intensity in tissue derived from affected versus unaffected dogs.

To assess collagen localization and discriminate between type I and type III collagens in ocular tissue, Picrosirius red staining of paraffin-embedded BH eye sections was conducted (Figure 5). Type I collagen indicated by orange, pink, and red hues was the predominant collagen type observed in all structures of the eye. When compared to a negative control stained with Mayer's Hematoxylin only, abundant localization of relatively thick, red-colored, type I collagen fibers was noted in the CB and the epithelial apical surface of the ciliary processes (Figure 5A). Similarly, strong type I collagen staining, appearing in red, was noted throughout the iris, cornea, and optic nerve (Figure 5B,C,D). On the other hand, reduced abundance in collagen deposition and fiber thickness were noted in the CC and TM, as indicated by the apparent orange-pink-colored fibers (Figure 5E). This finding validates the observed reduction in COL1A2 staining and localization in the TM shown above. Despite the

absence of obvious differences in the localization or intensity of collagen staining in affected versus unaffected derived tissue, an overall widespread localization of collagen was noted in all eye structures, thereby confirming its prominent expression in the eye.

DISCUSSION

Despite recent discoveries, the underlying genetic and environmental factors that contribute to the development and progression of glaucoma have not been fully elucidated. The condition may result in debilitating outcomes, including complete loss of vision in the absence of effective treatment. The identification of genetic variants that determine risk for developing glaucoma can not only be used to genetically identify dogs at low disease risk for breeding purposes, but may also provide insight into the pathophysiology of PACG.

GWA analysis of clinically confirmed BHs with PACG cases versus controls has led to the identification of two associated regions, which supports the role of a genetic component in modifying risk for PACG in the BH. The highest P_{genome} value was achieved for a susceptibility locus on chromosome 14 containing the genes *COL1A2* and *PEG10*. A second locus containing the gene *RAB22A* was identified on chromosome 24. SNPs marking both loci achieved P_{genome} values in the order of 10^{-4}, which indicates significant despite the modest sample size used. The observed pattern of haplotype distribution and allele frequency of markers within the loci identified does not support an additive effect of allele dosage in cases versus controls at multiple loci (Table 2 and Table 3). Based on these results, it appears that variation in multiple associated regions determines risk for canine PACG rather than a single, major locus. These observations highlight the complex nature of the genetic and environmental effects underlying PACG inheritance.

One shortcoming of this study is that in an effort to identify a sufficient number of clinically well-characterized dogs, animals from multiple PACG pedigrees were used. Additionally, cryptic relatedness is particularly common for dogs; a
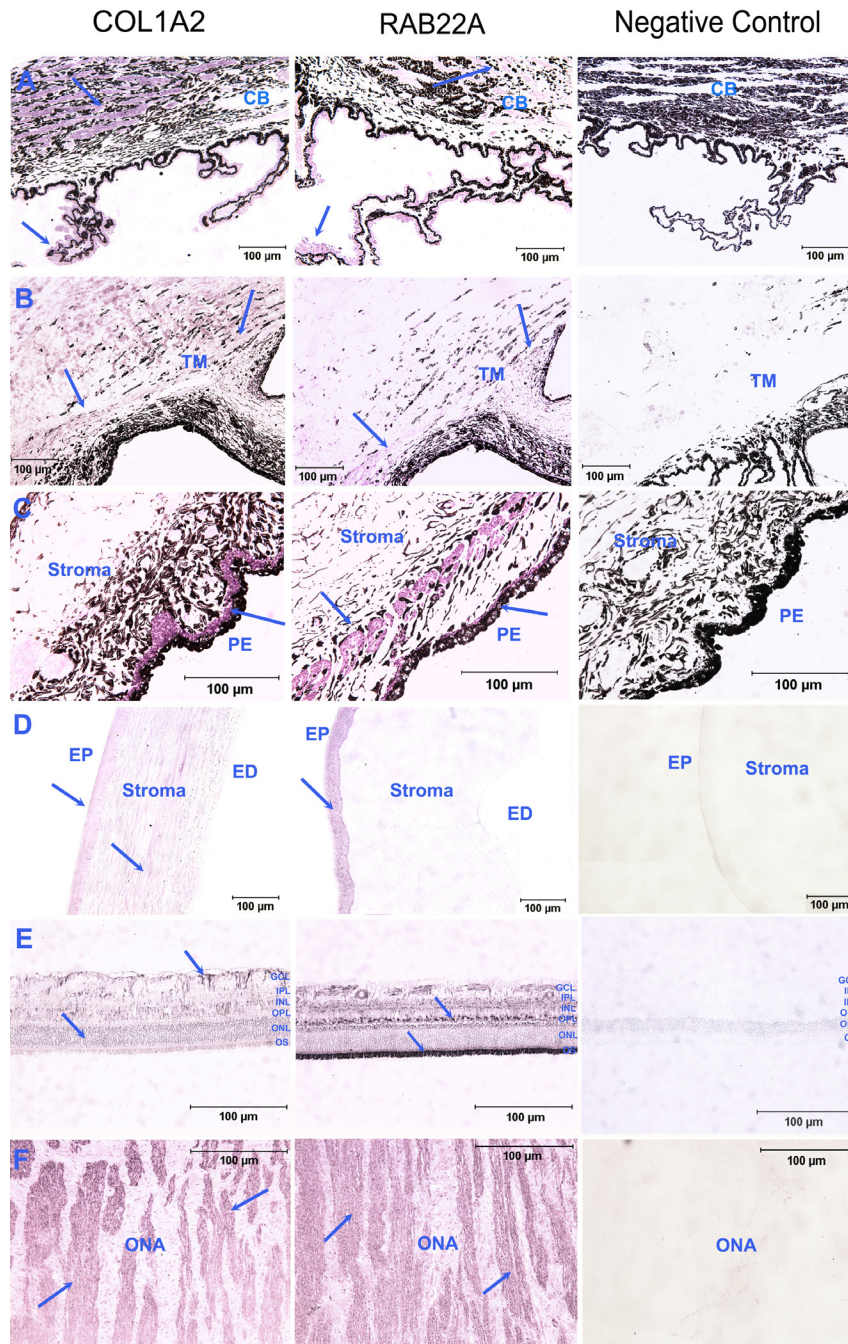
Figure 4. Immunohistochemistry staining for COL1A2 (left), RAB22A (middle), and negative control (primary antibody omitted; right) in sagittal sections of paraffin- embedded basset hound (BH) eyes derived from affected and unaffected animals. Variable intensities of COL1A2 and RAB22A staining were noted in the **A**: ciliary body (CB) and processes, **B**: trabecular meshwork (TM) and ciliary cleft (CC), **C**: stroma and pigmentary epithelium (PE) layers of the iris, **D**: epithelium (EP), stroma and endothelium (ED) layers of the cornea, **E**: retina (OS=outer segment, ONL=outer nuclear layer, OPL=outer plexiform layer, INL=inner nuclear layer, IPL=inner plexiform layer, GCL=ganglion cell layer; **E**), and **F**: optic nerve axons (ONA). Arrows indicate areas where staining was prominently observed.
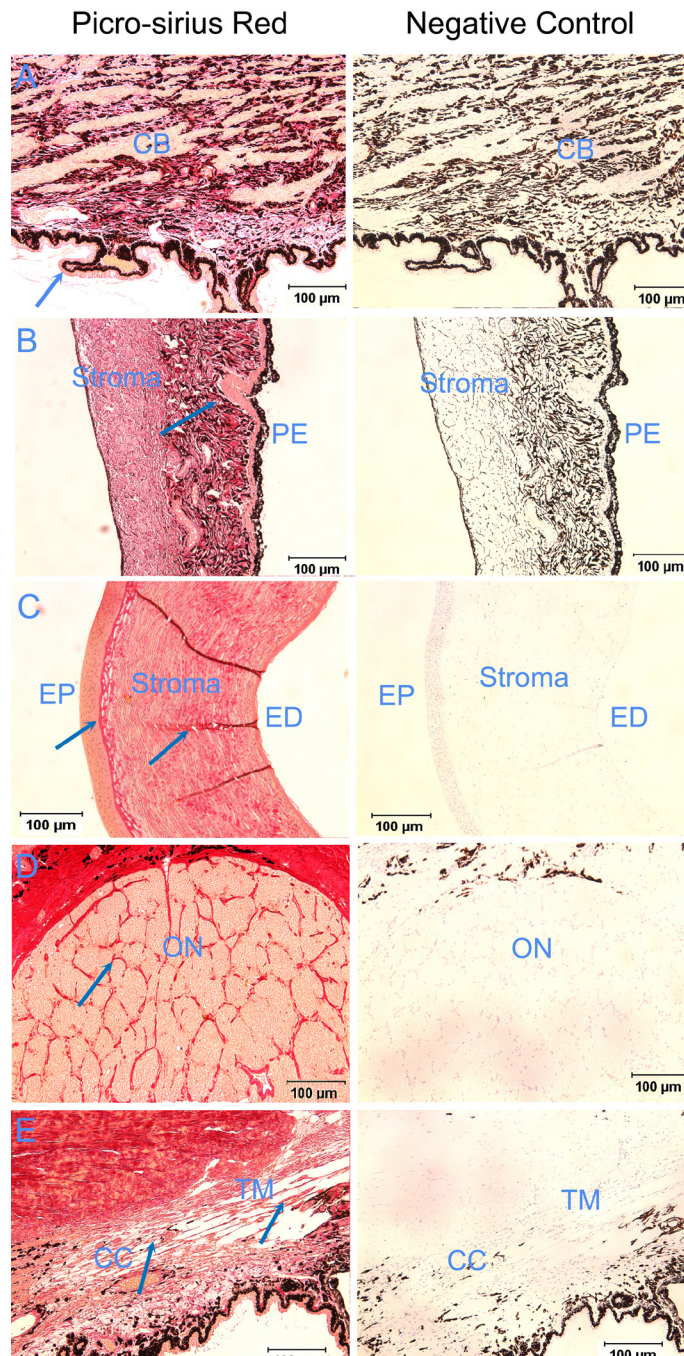
Figure 5. Picrosirius red (left) and negative control–Mayer's hematoxylin only (right) stained sagittal sections of paraffin-embedded basset hound (BH) eyes. Images were viewed using polarizing light microscopy. Collagen staining of fibers appears in hues of orange, pink, and red. The observed color intensity is indicative of collagen fiber thickness and abundance in tissue. Collagen fiber staining was noted in **A**: the ciliary body (CB) and processes, **B**: stroma and pigmentary epithelium (PE) layers of the iris, **C**: epithelium (EP), stroma and endothelium (ED) layers of the cornea, **D**: optic nerve (ON), **E**: ciliary cleft (CC) and trabecular meshwork (TM). Arrows indicate areas where staining was prominently observed, including the CB, iris, lens, and ON.

certain amount of relatedness is almost always detected, particularly in purebred dogs [22-24]. Sample independence is one of the main assumptions of most GWA test statistics [25,26], and thus the degree of relatedness among animals is a common concern in GWAS. However, a large number of animal studies were able to come to valid conclusions despite the discovery of cryptic relatedness among their study samples following the investigation of population stratification [22,23,27]. Herein, sample relatedness was addressed by selecting cases and controls that were as distantly related to each other as possible and by using statistical approaches to correct for confounding relatedness. Our results reveal the effectiveness of the statistical methods used here to resolve the confounding effects of cryptic relatedness initially observed among our samples.

Our findings also demonstrate that significant phenotype-genotype associations can be achieved with a modest sample size when using a closed and purebred population, such as the BH population used here. When compared to human populations, studies of the canine genome have shown that genetic homogeneity is much greater within individual dog breeds (94.6%) than within distinct human populations (72.5%) [28]. In some breeds, genetic variation has even been additionally reduced by extensive inbreeding and bottleneck events. The vast reduction in haplotype diversity in the dog genome facilitates mapping the genetic basis of phenotypic variation using GWAS [29,30]. Genetic associations can therefore be identified more efficiently using fewer markers and samples in canine versus human genetic studies [31]. With that in mind, the small sample size used in this study may be considered too modest to provide sufficient statistical power for detecting small genetic effects. This is particularly true if the risk variant is a rare allele with a small OR [32]. Human-based studies have demonstrated that when the causal SNP is rare (minor allele frequency [MAF]<10%), a sample size of 3,000 may still be underpowered to detect small genetic effects [33]. These findings may not be applicable to canine-based genetic studies considering the architecture of the canine genome, which could provide greater statistical power for the identification of risk variants with small effects using a smaller sample size relative to human-based studies [28].

It has been shown that many loci harboring common risk alleles for complex diseases will have effect sizes in the range of 1.1–1.2, which cannot be detected using the conventional study designs and sample sizes currently adopted, but rather using empirical analyses and significantly large sample sizes [34,35]. As such, our inability to detect small genetic effects with the sample size used here is expected considering that larger GWAS remain statistically underpowered to detect common variants with small effects. Our results reveal the strong association of two loci, containing promising candidate genes, to PACG. These findings support our expectation of detecting variants with large effects in association with a complex disease when using a small sample size.

Several research studies have provided convincing evidence of the potential role of collagen in glaucoma, making *COL1A2* a highly promising PACG candidate gene. Of particular interest is that a variant in the collagen gene *COL11A1* has been recently identified in a GWAS of human PACG [8]. Central corneal thickness (CCT) is a known and proven risk factor of glaucoma [36]. In a GWA study investigating CCT and brittle cornea syndrome in association with glaucoma, significant associations in the collagen genes *COL8A2* and *COL5A1* were identified [37]. These findings suggest a possible involvement of collagen genes in the pathogenesis of PACG. Moreover, analysis of AH collected from patients with POAG revealed increased fibroblast proliferation and collagen synthesis in POAG versus unaffected derived AH [38]. The increased rate of fibroblast activity is speculated to contribute to excess deposition of collagen and subsequent loss of the TM cells during the development of glaucoma [38]. In addition, this locus contains a second gene—*PEG10*. Little is known about this gene, but studies in the mouse demonstrate that it is an imprinted, retrotransposon-derived gene. *Peg10* knockout mice showed early embryonic lethality, which indicates its critical role in mouse development [39]. Ras-related Protein *RAB22A*, a member of the RAB family of small GTPases was identified within the second PACG associated locus in the BH. The protein encoded by this gene has been shown to interact with early-endosomal antigen 1, and may be involved in the trafficking of molecules between endosomal compartments [40]. Neither *PEG10* nor *RAB22A* has been discussed in relation to the pathology of glaucoma in the past.

In conclusion, we have identified two loci associated with PACG in the BH. Our findings indicate the possible involvement of a collagen-related mechanism in the development of glaucoma in the BH. This finding is in accordance with emerging data that support the role of collagen in human PACG. Additional functional studies will be required to investigate the role of *COL1A2* and possibly other collagen-encoding genes in PACG. This GWA analysis of genetic associations has demonstrated the complexity of PACG by implicating several genetic loci in association with the disease. Sequencing of candidate genes within the identified disease-associated loci will possibly lead to the identification of PACG-causing mutations in the BH. In addition to

identifying the genetic variants underlying the disease, understanding the environmental factors that potentially modify risk to glaucoma is crucial for characterizing the pathophysiology of PACG. Ultimately, we anticipate the utilization of our findings in estimating disease risk in susceptible BHs and possibly other dog breeds susceptible to PACG. This finding may contribute to the reduction of disease incidence in the BH by selectively breeding animals following genetic testing for risk variants. With further research, findings in this study may shed light on important molecular mechanisms that contribute to PACG in the canine and potentially human patients.

ACKNOWLEDGMENTS

REFERENCES

1. Quigley HA, Broman AT. The number of people with glaucoma worldwide in 2010 and 2020. Br J Ophthalmol 2006; 90:262-7. [PMID: 16488940].

2. Foster PJ, Baasanhu J, Alsbirk PH, Munkhbayar D, Uranchimeg D, Johnson GJ. Glaucoma in Mongolia. A population-based survey in Hovsgol province, northern Mongolia. Arch Ophthalmol 1996; 114:1235-41. [PMID: 8859083].

3. Foster PJ, Oen FT, Machin D, Ng TP, Devereux JG, Johnson GJ, Khaw PT, Seah SK. The prevalence of glaucoma in Chinese residents of Singapore: a cross-sectional population survey of the Tanjong Pagar district. Arch Ophthalmol 2000; 118:1105-11. [PMID: 10922206].

4. Dandona L, Dandona R, Mandal P, Srinivas M, John RK, McCarty CA, Rao GN. Angle-closure glaucoma in an urban population in southern India. The Andhra Pradesh eye disease study. Ophthalmology 2000; 107:1710-6. [PMID: 10964834].

5. Grozdanic SD, Kecova H, Harper MM, Nilaweera W, Kuehn MH, Kardon RH. Functional and structural changes in a canine model of hereditary primary angle-closure glaucoma. Invest Ophthalmol Vis Sci 2010; 51:255-63. [PMID: 19661222].

6. Jiang B, Harper MM, Kecova H, Adamus G, Kardon RH, Grozdanic SD, Kuehn MH. Neuroinflammation in advanced canine glaucoma. Mol Vis 2010; 16:2092-108. [PMID: 21042562].

7. Nair KS, Hmani-Aifa M, Ali Z, Kearney AL, Ben Salem S, Macalinao DG, Cosma IM, Bouassida W, Hakim B, Benzina Z, Soto I, Soderkvist P, Howell GR, Smith RS, Ayadi H, John SW. Alteration of the serine protease PRSS56 causes angle-closure glaucoma in mice and posterior microphthalmia

in humans and mice. Nat Genet 2011; 43:579-84. [PMID: 21532570].

8. Vithana EN, Khor CC, Qiao C, Nongpiur ME, George R, Chen LJ, Do T, Abu-Amero K, Huang CK, Low S, Tajudin LS, Perera SA, Cheng CY, Xu L, Jia H, Ho CL, Sim KS, Wu RY, Tham CC, Chew PT, Su DH, Oen FT, Sarangapani S, Soumittra N, Osman EA, Wong HT, Tang G, Fan S, Meng H, Huong DT, Wang H, Feng B, Baskaran M, Shantha B, Ramprasad VL, Kumaramanickavel G, Iyengar SK, How AC, Lee KY, Sivakumaran TA, Yong VH, Ting SM, Li Y, Wang YX, Tay WT, Sim X, Lavanya R, Cornes BK, Zheng YF, Wong TT, Loon SC, Yong VK, Waseem N, Yaakub A, Chia KS, Allingham RR, Hauser MA, Lam DS, Hibberd ML, Bhattacharya SS, Zhang M, Teo YY, Tan DT, Jonas JB, Tai ES, Saw SM. Hon do N, Al-Obeidan SA, Liu J, Chau TN, Simmons CP, Bei JX, Zeng YX, Foster PJ, Vijaya L, Wong TY, Pang CP, Wang N, Aung T. Genome-wide association analyses identify three new susceptibility loci for primary angle closure glaucoma. Nat Genet 2012; 44:1142-6. [PMID: 22922875].

9. Alsbirk PH. Anterior chamber depth and primary angle-closure glaucoma. II. A genetic study. Acta Ophthalmol (Copenh) 1975; 53:436-49. [PMID: 1174403].

10. Alsbirk PH. Anterior chamber depth and primary angle-closure glaucoma. I. An epidemiologic study in Greenland Eskimos. Acta Ophthalmol (Copenh) 1975; 53:89-104. [PMID: 1172916].

11. Cong Y, Guo X, Liu X, Cao D, Jia X, Xiao X, Li S, Fang S, Zhang Q. Association of the single nucleotide polymorphisms in the extracellular matrix metalloprotease-9 gene with PACG in southern China. Mol Vis 2009; 15:1412-7. [PMID: 19633731].

12. Awadalla MS, Burdon KP, Kuot A, Hewitt AW, Craig JE. Matrix metalloproteinase-9 genetic variation and primary angle closure glaucoma in a Caucasian population. Mol Vis 2011; 17:1420-4. [PMID: 21655354].

13. Aung T, Yong VH, Lim MC, Venkataraman D, Toh JY, Chew PT, Vithana EN. Lack of association between the rs2664538 polymorphism in the MMP-9 gene and primary angle closure glaucoma in Singaporean subjects. J Glaucoma 2008; 17:257-8. [PMID: 18552608].

14. Kuchtey J, Olson LM, Rinkoski T, Mackay EO, Iverson TM, Gelatt KN, Haines JL, Kuchtey RW. Mapping of the disease locus and identification of ADAMTS10 as a candidate gene in a canine model of primary open angle glaucoma. PLoS Genet 2011; 7:e1001306-[PMID: 21379321].

15. Ahonen SJ, Pietila E, Mellersh CS, Tiira K, Hansen L, Johnson GS, Lohi H. Genome-wide association study identifies a novel canine glaucoma locus. PLoS ONE 2013; 8:e70903-[PMID: 23951034].

16. Firasat S, Riazuddin SA, Hejtmancik JF, Riazuddin S. Primary congenital glaucoma localizes to chromosome 14q24.2–24.3 in two consanguineous Pakistani families. Mol Vis 2008; 14:1659-65. [PMID: 18776954].

17. Gelatt KN, Brooks DE, Samuelson DA. Comparative glaucomatology. I: The spontaneous glaucomas. J Glaucoma 1998; 7:187-201. [PMID: 9627859].

18. Gelatt KN, MacKay EO. Prevalence of the breed-related glaucomas in pure-bred dogs in North America. Vet Ophthalmol 2004; 7:97-111. [PMID: 14982589].

19. Purcell S, Neale B, Todd-Brown K, Thomas L, Ferreira MA, Bender D, Maller J, Sklar P, de Bakker PI, Daly MJ, Sham PC. PLINK: a tool set for whole-genome association and population-based linkage analyses. Am J Hum Genet 2007; 81:559-75. [PMID: 17701901].

20. Zhu C, Yu J. Nonmetric multidimensional scaling corrects for population structure in association mapping with different sample types. Genetics 2009; 182:875-88. [PMID: 19414565].

21. Price AL, Zaitlen NA, Reich D, Patterson N. New approaches to population stratification in genome-wide association studies. Nat Rev Genet 2010; 11:459-63. [PMID: 20548291].

22. Tengvall K, Kierczak M, Bergvall K, Olsson M, Frankowiack M, Farias FH, Pielberg G, Carlborg O, Leeb T, Andersson G, Hammarstrom L, Hedhammar A, Lindblad-Toh K. Genome-wide analysis in German shepherd dogs reveals association of a locus on CFA 27 with atopic dermatitis. PLoS Genet 2013; 9:e1003475-[PMID: 23671420].

23. Mogensen MS, Karlskov-Mortensen P, Proschowsky HF, Lingaas F, Lappalainen A, Lohi H, Jensen VF, Fredholm M. Genome-wide association study in Dachshund: identification of a major locus affecting intervertebral disc calcification. J Hered 2011; 102:Suppl 1S81-6. [PMID: 21846751].

24. Owczarek-Lipska M, Lauber B, Molitor V, Meury S, Kierczak M, Tengvall K, Webster MT, Jagannathan V, Schlotter Y, Willemse T, Hendricks A, Bergvall K, Hedhammar A, Andersson G, Lindblad-Toh K, Favrot C, Roosje P, Marti E, Leeb T. Two loci on chromosome 5 are associated with serum IgE levels in Labrador retrievers. PLoS ONE 2012; 7:e39176-[PMID: 22720065].

25. Stranger BE, Stahl EA, Raj T. Progress and promise of genome-wide association studies for human complex trait genetics. Genetics 2011; 187:367-83. [PMID: 21115973].

26. Bush WS, Moore JH. Chapter 11: Genome-wide association studies. PLOS Comput Biol 2012; 8:e1002822-[PMID: 23300413].

27. Ma L, Wiggans GR, Wang S, Sonstegard TS, Yang J, Crooker BA, Cole JB, Van Tassell CP, Lawlor TJ, Da Y. Effect of sample stratification on dairy GWAS results. BMC Genomics 2012; 13:536-[PMID: 23039970].

28. Ostrander EA, Wayne RK. The canine genome. Genome Res 2005; 15:1706-16. [PMID: 16339369].

29. Vaysse A, Ratnakumar A, Derrien T, Axelsson E, Rosengren Pielberg G, Sigurdsson S, Fall T, Seppala EH, Hansen MS, Lawley CT, Karlsson EK, Bannasch D, Vila C, Lohi H, Galibert F, Fredholm M, Haggstrom J, Hedhammar A, Andre C, Lindblad-Toh K, Hitte C, Webster MT. Identification of genomic regions associated with phenotypic variation between dog breeds using selection mapping. PLoS Genet 2011; 7:e1002316-[PMID: 22022279].

30. Sutter NB, Eberle MA, Parker HG, Pullar BJ, Kirkness EF, Kruglyak L, Ostrander EA. Extensive and breed-specific linkage disequilibrium in Canis familiaris. Genome Res 2004; 14:2388-96. [PMID: 15545498].

31. Lindblad-Toh K, Wade CM, Mikkelsen TS, Karlsson EK, Jaffe DB, Kamal M, Clamp M, Chang JL, Kulbokas EJ 3rd, Zody MC, Mauceli E, Xie X, Breen M, Wayne RK, Ostrander EA, Ponting CP, Galibert F, Smith DR, DeJong PJ, Kirkness E, Alvarez P, Biagi T, Brockman W, Butler J, Chin CW, Cook A, Cuff J, Daly MJ, DeCaprio D, Gnerre S, Grabherr M, Kellis M, Kleber M, Bardeleben C, Goodstadt L, Heger A, Hitte C, Kim L, Koepfli KP, Parker HG, Pollinger JP, Searle SM, Sutter NB, Thomas R, Webber C, Baldwin J, Abebe A, Abouelleil A, Aftuck L, Ait-Zahra M, Aldredge T, Allen N, An P, Anderson S, Antoine C, Arachchi H, Aslam A, Ayotte L, Bachantsang P, Barry A, Bayul T, Benamara M, Berlin A, Bessette D, Blitshteyn B, Bloom T, Blye J, Boguslavskiy L, Bonnet C, Boukhgalter B, Brown A, Cahill P, Calixte N, Camarata J, Cheshatsang Y, Chu J, Citroen M, Collymore A, Cooke P, Dawoe T, Daza R, Decktor K, DeGray S, Dhargay N, Dooley K, Dooley K, Dorje P, Dorjee K, Dorris L, Duffey N, Dupes A, Egbiremolen O, Elong R, Falk J, Farina A, Faro S, Ferguson D, Ferreira P, Fisher S, FitzGerald M, Foley K, Foley C, Franke A, Friedrich D, Gage D, Garber M, Gearin G, Giannoukos G, Goode T, Goyette A, Graham J, Grandbois E, Gyaltsen K, Hafez N, Hagopian D, Hagos B, Hall J, Healy C, Hegarty R, Honan T, Horn A, Houde N, Hughes L, Hunnicutt L, Husby M, Jester B, Jones C, Kamat A, Kanga B, Kells C, Khazanovich D, Kieu AC, Kisner P, Kumar M, Lance K, Landers T, Lara M, Lee W, Leger JP, Lennon N, Leuper L, LeVine S, Liu J, Liu X, Lokyitsang Y, Lokyitsang T, Lui A, Macdonald J, Major J, Marabella R, Maru K, Matthews C, McDonough S, Mehta T, Meldrim J, Melnikov A, Meneus L, Mihalev A, Mihova T, Miller K, Mittelman R, Mlenga V, Mulrain L, Munson G, Navidi A, Naylor J, Nguyen T, Nguyen N, Nguyen C, Nguyen T, Nicol R, Norbu N, Norbu C, Novod N, Nyima T, Olandt P, O'Neill B, O'Neill K, Osman S, Oyono L, Patti C, Perrin D, Phunkhang P, Pierre F, Priest M, Rachupka A, Raghuraman S, Rameau R, Ray V, Raymond C, Rege F, Rise C, Rogers J, Rogov P, Sahalie J, Settipalli S, Sharpe T, Shea T, Sheehan M, Sherpa N, Shi J, Shih D, Sloan J, Smith C, Sparrow T, Stalker J, Stange-Thomann N, Stavropoulos S, Stone C, Stone S, Sykes S, Tchuinga P, Tenzing P, Tesfaye S, Thoulutsang D, Thoulutsang Y, Topham K, Topping I, Tsamla T, Vassiliev H, Venkataraman V, Vo A, Wangchuk T, Wangdi T, Weiand M, Wilkinson J, Wilson A, Yadav S, Yang S, Yang X, Young G, Yu Q, Zainoun J, Zembek L, Zimmer A, Lander ES. Genome sequence, comparative analysis and haplotype structure of the domestic dog. Nature 2005; 438:803-19. [PMID: 16341006].

32. Marchini J, Howie B, Myers S, McVean G, Donnelly P. A new multipoint method for genome-wide association studies by imputation of genotypes. Nat Genet 2007; 39:906-13. [PMID: 17572673].

33. Spencer CC, Su Z, Donnelly P, Marchini J. Designing genome-wide association studies: sample size, power, imputation, and the choice of genotyping chip. PLoS Genet 2009; 5:e1000477-[PMID: 19492015].

34. Zeggini E, Scott LJ, Saxena R, Voight BF, Marchini JL, Hu T, de Bakker PI, Abecasis GR, Almgren P, Andersen G, Ardlie K, Bostrom KB, Bergman RN, Bonnycastle LL, Borch-Johnsen K, Burtt NP, Chen H, Chines PS, Daly MJ, Deodhar P, Ding CJ, Doney AS, Duren WL, Elliott KS, Erdos MR, Frayling TM, Freathy RM, Gianniny L, Grallert H, Grarup N, Groves CJ, Guiducci C, Hansen T, Herder C, Hitman GA, Hughes TE, Isomaa B, Jackson AU, Jorgensen T, Kong A, Kubalanza K, Kuruvilla FG, Kuusisto J, Langenberg C, Lango H, Lauritzen T, Li Y, Lindgren CM, Lyssenko V, Marvelle AF, Meisinger C, Midthjell K, Mohlke KL, Morken MA, Morris AD, Narisu N, Nilsson P, Owen KR, Palmer CN, Payne F, Perry JR, Pettersen E, Platou C, Prokopenko I, Qi L, Qin L, Rayner NW, Rees M, Roix JJ, Sandbaek A, Shields B, Sjogren M, Steinthorsdottir V, Stringham HM, Swift AJ, Thorleifsson G, Thorsteinsdottir U, Timpson NJ, Tuomi T, Tuomilehto J, Walker M, Watanabe RM, Weedon MN, Willer CJ, Illig T, Hveem K, Hu FB, Laakso M, Stefansson K, Pedersen O, Wareham NJ, Barroso I, Hattersley AT, Collins FS, Groop L, McCarthy MI, Boehnke M, Altshuler D. Meta-analysis of genome-wide association data and large-scale replication identifies additional susceptibility loci for type 2 diabetes. Nat Genet 2008; 40:638-45. [PMID: 18372903].

35. Barrett JC, Hansoul S, Nicolae DL, Cho JH, Duerr RH, Rioux JD, Brant SR, Silverberg MS, Taylor KD, Barmada MM, Bitton A, Dassopoulos T, Datta LW, Green T, Griffiths AM, Kistner EO, Murtha MT, Regueiro MD, Rotter JI, Schumm LP, Steinhart AH, Targan SR, Xavier RJ, Libioulle C, Sandor C, Lathrop M, Belaiche J, Dewit O, Gut I, Heath S, Laukens D, Mni M, Rutgeerts P, Van Gossum A, Zelenika D, Franchimont D, Hugot JP, de Vos M, Vermeire S, Louis E, Cardon LR, Anderson CA, Drummond H, Nimmo E, Ahmad T, Prescott NJ, Onnie CM, Fisher SA, Marchini J, Ghori J, Bumpstead S, Gwilliam R, Tremelling M, Deloukas P, Mansfield J, Jewell D, Satsangi J, Mathew CG, Parkes M, Georges M, Daly MJ. Genome-wide association defines more than 30 distinct susceptibility loci for Crohn's disease. Nat Genet 2008; 40:955-62. [PMID: 18587394].

36. Freeman EE, Roy-Gagnon MH, Descovich D, Masse H, Lesk MR. The heritability of glaucoma-related traits corneal hysteresis, central corneal thickness, intraocular pressure, and choroidal blood flow pulsatility. PLoS ONE 2013; 8:e55573-[PMID: 23383229].

37. Vithana EN, Aung T, Khor CC, Cornes BK, Tay WT, Sim X, Lavanya R, Wu R, Zheng Y, Hibberd ML, Chia KS, Seielstad M, Goh LK, Saw SM, Tai ES, Wong TY. Collagen-related genes influence the glaucoma risk factor, central corneal thickness. Hum Mol Genet 2011; 20:649-58. [PMID: 21098505].

38. González-Avila G, Ginebra M, Hayakawa T, Vadillo-Ortega F, Teran L, Selman M. Collagen metabolism in human aqueous humor from primary open-angle glaucoma. Decreased degradation and increased biosynthesis play a role in its pathogenesis. Arch Ophthalmol 1995; 113:1319-23. [PMID: 7575267].

39. Ono R, Nakamura K, Inoue K, Naruse M, Usami T, Wakisaka-Saito N, Hino T, Suzuki-Migishima R, Ogonuki N, Miki H, Kohda T, Ogura A, Yokoyama M, Kaneko-Ishino T, Ishino F. Deletion of Peg10, an imprinted gene acquired from a retrotransposon, causes early embryonic lethality. Nat Genet 2006; 38:101-6. [PMID: 16341224].

40. Magadán JG, Barbieri MA, Mesa R, Stahl PD, Mayorga LS. Rab22a regulates the sorting of transferrin to recycling endosomes. Mol Cell Biol 2006; 26:2595-614. [PMID: 16537905].